symmetry

MDPI

Article

Appropriate Feature Set and Window Parameters Selection for Efficient Motion Intent Characterization towards Intelligently Smart EMG-PR System

Mojisola Grace Asogbon [1,2,†], Oluwarotimi Williams Samuel [1,2,†], Yanbing Jiang [1,2], Lin Wang [1], Yanjuan Geng [1,2], Arun Kumar Sangaiah [3], Shixiong Chen [1,2], Peng Fang [1,2] and Guanglin Li [1,2,4,*]

1 CAS Key Laboratory of Human-Machine Intelligence-Synergy Systems, Shenzhen Institutes of Advanced Technology (SIAT), Chinese Academy of Sciences (CAS), Shenzhen 518055, China; grace@siat.ac.cn (M.G.A.); samuel@siat.ac.cn (O.W.S.); yb.jiang@siat.ac.cn (Y.J.); lin.wang1@siat.ac.cn (L.W.); yj.geng@siat.ac.cn (Y.G.); sx.chen@siat.ac.cn (S.C.); peng.fang@siat.ac.cn (P.F.)

2 Shenzhen College of Advanced Technology, University of Chinese Academy of Sciences, Shenzhen 518055, China

3 School of Computing Science and Engineering, VIT University, Vellore 632014, Tamil Nadu, India; sarunkumar@vit.ac.in

4 SIAT Branch, Shenzhen Institute of Artificial Intelligence and Robotics for Society, CAS, Shenzhen 518055, China

* Correspondence: gl.li@siat.ac.cn

† These authors contributed equally to this work.

Received: 13 September 2020; Accepted: 12 October 2020; Published: 16 October 2020

Abstract: The constantly rising number of limb stroke survivors and amputees has motivated the development of intelligent prosthetic/rehabilitation devices for their arm function restoration. The device often integrates a pattern recognition (PR) algorithm that decodes amputees' limb movement intent from electromyogram (EMG) signals, characterized by neural information and symmetric distribution. However, the control performance of the prostheses mostly rely on the interrelations among multiple dynamic factors of feature set, windowing parameters, and signal conditioning that have rarely been jointly investigated to date. This study systematically investigated the interaction effects of these dynamic factors on the performance of EMG-PR system towards constructing optimal parameters for accurately robust movement intent decoding in the context of prosthetic control. In this regard, the interaction effects of various features across window lengths (50 ms~300 ms), increments (50 ms~125 ms), robustness to external interferences and sensor channels (2 ch~6 ch), were examined using EMG signals obtained from twelve subjects through a symmetrical movement elicitation protocol. Compared to single features, multiple features consistently achieved minimum decoding error below 10% across optimal windowing parameters of 250 ms/100 ms. Also, the multiple features showed high robustness to additive noise with obvious trade-offs between accuracy and computation time. Consequently, our findings may provide proper insight for appropriate parameter selection in the context of robust PR-based control strategy for intelligent rehabilitation device.

Keywords: rehabilitation device; electromyogram; symmetry; window parameters; feature extraction; pattern recognition

1. Introduction

Individuals with limb amputation or congenital limb deficits or stroke often have difficulty in performing simple and complex daily life activities that involve the use of their upper extremity (UE).

They often depend on the healthy part of their body to compensate for a lost limb, which can greatly affect body posture and symmetry alignment. They also experience phantom limb sensation (which is usually painful), fatigue, and depression among others, which can cause emotional and psychological damage. In addition, majority of individuals with UE disability normally feel inferior or perhaps rejected in the society because they can hardly cope with certain physical daily life activities [1–3].

Re-integrating this category of persons into the society would require the development of a smart and intelligent rehabilitation robotic system [2–5]. Such intelligent robotic system normally incorporate less computational control algorithms that operate on symmetric principle and attract low memory and processor requirement, thus, aiding the realization of portable rehabilitation device that could be worn by amputees to help restore their arm functions [3–6]. Notably, such symmetrical principle play a significant role when it comes to the dynamics of controlling the prosthetic device during activities of daily living [7]. At the forefront of this technology is the pattern recognition based prostheses that seamlessly decode multiple patterns of targeted limb movements from measured bioelectrical data and provide multiple degrees of freedom arm function in an intuitive fashion [1,3,4]. Typically, the pattern recognition strategy involves extraction of highly informative feature sets from the measured surface electromyogram (sEMG) data, which are applied to a machine learning model for limb movement intent decoding.

Afterwards, the deciphered movement intents are coded into control commands that drives the intelligently smart prostheses in a way similar to the natural human arm [6–10]. The pattern recognition based control strategy consist of sequentially connected phases in which the machine learning algorithm and feature extraction phases are well-thought-out as important with the latter being the most significant. Hence, the feature extraction approach adopted would either potentially improve or degrade the overall performance of device, and it has been proven by several previous studies [5,11,12]. In other words, developing an intelligently smart pattern recognition based prostheses would require the integration of appropriate feature extraction technique. Moreover, extracting features from segmented sEMG data as against the entire length of measured data would expedite the response rate of the prosthetic device in real-life applications, and the sliding window segmentation technique has been widely employed due to its dense decision stream attribute [13]. Integral elements of the sliding window segmentation scheme includes the window length and increment parameters, which would normally influence the characteristics of the extracted feature set (in terms of stability and accuracy) [12,13]. These parameters have direct impact on the extracted features and as well influence the characteristics of the prostheses controller in terms of its delay, since the delay is a function of the computation time associated with the extracted features [14,15]. Therefore, the overall effect of the feature extraction scheme and windowing parameters should not be underestimated if the goal is to realize an intelligently smart prostheses that would be clinically viable. Towards addressing the above highlighted problem, Menon et al. examined the effect of sliding window segmentation on classification accuracy using sEMG data measured from different groups of participants (able-bodied, partial hand and transhumeral participants). They found that the impact of window length on classification performance does not depend on the number of electrodes channels irrespective of the participants group. It was also discovered that the window increment has no direct effect on the classification accuracy regardless of the window length, number of electrode channels considered and the amputation status of participants, [16]. Meanwhile, in the Englehart and Hudgins study, they demonstrated the relationship between the analysis window length and classification error and it was realized that the mean classification error increase with short window length [13]. Smith et al. in their work investigated the relationship between window length, classification accuracy and controller delay and their result showed that the choice of window length is an important factor that could, either improve or degrade the performance of pattern recognition based prostheses control [14]. Other researchers demonstrated that to realize acceptable accuracy with reasonable controller delay, window lengths in the range of 100 ms~125 ms should be considered and that the controller delay in real-time operation should be lower than 200 ms. Also, window lengths between the range of 100 ms~300 ms [12],

and 300 ms~400 ms [13] were previously recommended [17–21]. However, no singular study has considered investigating the interrelation effects amongst classification accuracy, computation time, robustness to external noise, and number of electrode channels, across different window parameters and multiple feature sets for EMG-Pattern recognition (EMG-PR) systems. In other words, it is unclear how these multiple dynamic factors would influence movement intent decoding, which represent an essential control input for intelligently smart EMG-PR based prostheses. Additionally, investigations on the tradeoff amongst these factors across combinations of window parameters and feature sets has seldom been considered particularly when using sEMG recordings from amputees for movement intent decoding, thus, constituting a core research gap in the field of intelligently smart prostheses.

In this study, we systematically investigated the interrelations and impact of various windowing parameters on a range of feature sets when applied to decode multiple-patterns of targeted limb movement intents across amputees (who are the final users of the prosthetic device) and healthy subjects. Afterwards, the performance evaluation of the extracted features were carried out with respect to classification error, computation time, robustness to external noise and number of recording channels, in the context of machine learning based EMG-PR movement intent classifier.

Interestingly, the experiment and analyses were conducted using sEMG data acquired from both able-bodied-subjects, transradial, and transhumeral amputees, which would ensure the potential application of the study outcomes in clinical and commercial settings. The main contributions of this study are in three folds:

1. Towards providing a standard guideline that would aid the development of intelligently intuitive and symmetric prosthesis for upper limb amputees, this study systematically investigated the interrelations of multiple dynamic factors (windowing parameters, signal conditioning, and feature sets) on the movement intent decoding performance of EMG-PR system based on Linear Discriminant Analysis (LDA). It is worth noting that this issue has rarely been investigated to date.
2. A framework for optimal feature set and windowing parameter (window length and increment) construction in context of movement intent decoding was established. This enables the identification of features with low computation and high discrimination capability alongside their corresponding windowing parameters for both amputees and healthy subjects.
3. Further, the tradeoff between the decoding accuracy of a range of feature sets and their computational complexity across a combination of window parameters was examined with the aim of triggering positive development in the field of smart prosthetic control system and other pattern recognition-based systems that focus on providing smart healthcare services.

In summary, the outcomes of this study are capable of providing researchers and developers with proper insight on how to best select features and/or windowing parameters to achieve optimal movement intent decoding in EMG pattern recognition systems. Furthermore, it may spur potential advancement in smart prosthetic control system and other areas that employs pattern recognition based concept for the provision of smart healthcare services [22–24].

2. Materials and Methods

The EMG-PR framework, adopted in this study, is shown in Figure 1. The process begins with the acquisition of the EMG signals, followed by the preprocessing of the signals to remove motion artifacts and power line interference. The resulting filtered EMG signal is segmented using a sliding analysis window technique. This step is often recommended to improve the efficiency of the subsequent processes which typical involves feature extraction and classification. Thereafter, each feature extraction method, considered in this study, is extracted from the analysis window, and the classifier is employed to decode the motion intent based on the extracted features.

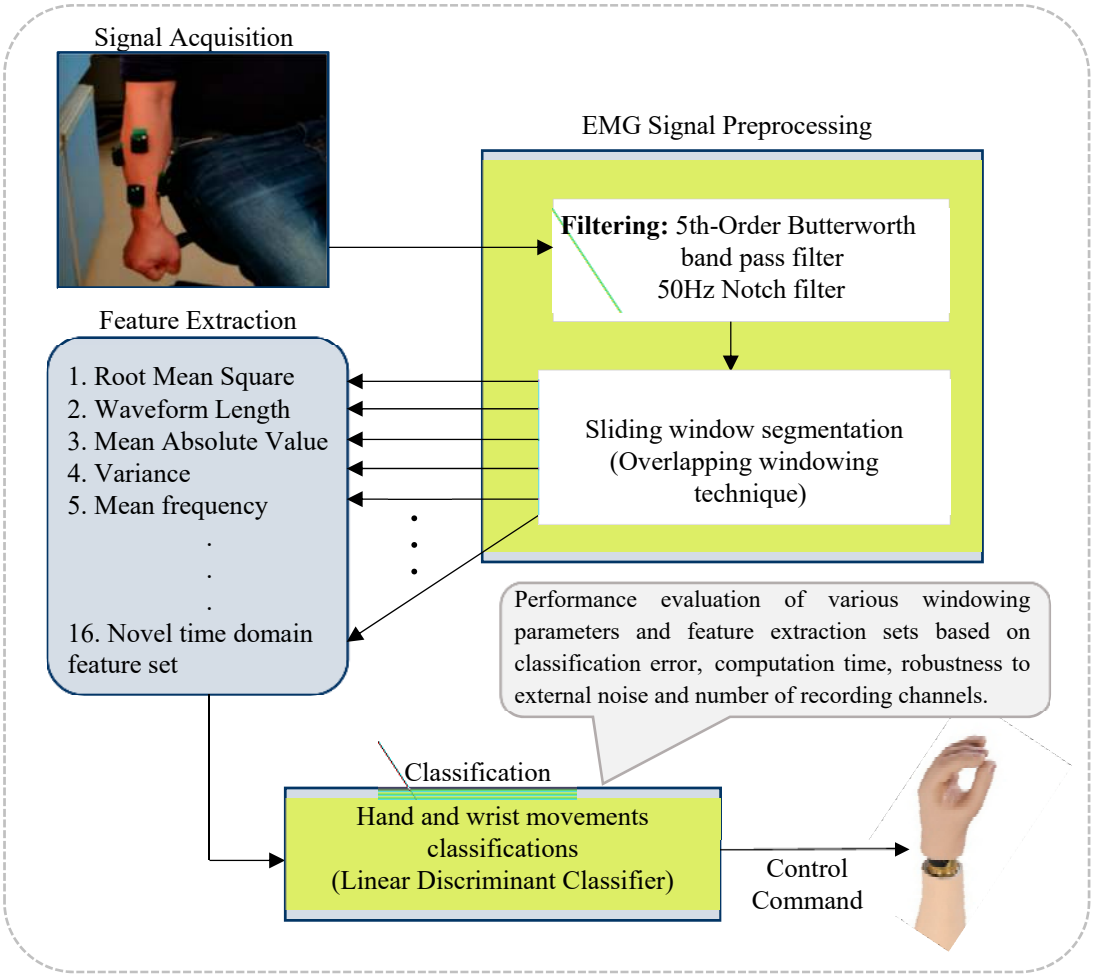

Figure 1. The block diagram of the electromyogram based pattern recognition control model.

2.1. Participant Information

In this study, a total of twelve subjects participated in the sEMG data measurement experiments. Five out of the recruited participants are fully-limbed subjects also referred to as able-bodied subjects while the remaining seven are arm amputees. Their ages range between 20~28 years and they all right-hand dominated. For the seven amputees, five of them had transradial amputation while the other two had transhumeral amputation. Prior to their inclusion in the study, their residual limbs were carefully examined to ensure appropriate conformity with the study objectives. Firstly, their residual limb muscles were carefully checked to ensure that they had no neuromuscular disorder. Secondly, the amputees were asked to perform a number targeted limb movements in a random sequence during which the myoelectric activities of their residual muscles were visualized, and afterwards certifies as being okay. Meanwhile, the amputees all have unilateral amputation with three of them having core experience in the usage of myoelectrically driven prostheses. Prior to the commencement of this experiment, the subjects were made to understand the aim of study, and they all consented and gave permission for the publication of their photographs/data for scientific purposes. Afterwards, the study protocol was approved by the Shenzhen Institutes of Advanced Technology Institutional Review Board, Chinese Academy of Sciences, China.

2.2. EMG Data Measurement

The commonly utilized sEMG data recording device known as Trigno wireless recording system (Developed by Delsys Inc., a company based in Boston, MA, USA) was employed for the acquisition of

the required sEMG signals. To determine the number of needed sEMG electrodes, we firstly examined different electrode configurations that involved the placement of 4~8 sensors on the forearm region. Afterwards, we realized that a total of six sensors would be sufficient to acquire high-quality recordings from which multiple-patterns of targeted limb movements could be adequately decoded. Each of the sensor contains 4 silver-bars that integrates three-axis accelerometer to capture arm dynamics and mechanomyogram signals. Meanwhile, the six sensors were configured to measure only sEMG without capturing the eighteen-channel mechanomyogram data, since we are only interested in analyzing the participants' limb movement intent from the sEMG signals. Although, there are other EMG measurement devices, but we decided to use the Trigno wireless recording system because it easy to use, it allows the recorded signals to be visualized in real-time which enables us to assess the signal quality, and it has wireless capability, that does not constrain the subjects during the experiment.

Haven determined the electrode configurations, the placement of the sensors was preceded by palpation of the remaining arm muscles in the amputee subjects to locate their belly and length as indicated in previous studies [24,25]. Afterwards, the sensors were placed over the skin area underlying the identified arm muscles in a symmetrical manner across both arms with the aid of adhesive (Figure 2a). That is, two out of the six sEMG sensors were placed on the extensor and flexor arm muscles while the remaining four sensors were positioned about 2–3 cm around the elbow crease as shown in Figure 2a,b. Notably, the symmetrical concept adopted in placing the electrode across both arms would enable the participant's intact arm to guide the amputated arm in adequately eliciting their movement intent during the experiment, which would lead to the recording of EMG signals with high neural information for movement intent decoding (Figure 2a). Prior to the sensor placement, the sensor sites mapped out on the participants' skin surface were thoroughly wiped using alcohol pads that takes off dry-dermis and skin-oil, which may affect the recorded signal's quality. For participants with unduly dry skin, the skin cells were extricated via tapping of the site with medical tapes to guarantee good electrode-skin contact. After ensuring proper electrode placement and good experimental condition, the subjects were presented with an audio prompt to guide them in performing all the classes of targeted upper-limb movements in a sequential order that includes: wrist movements (wrist flexion/extension/pronation/supination), hand movements (hand close/open) as shown in Figure 2c.

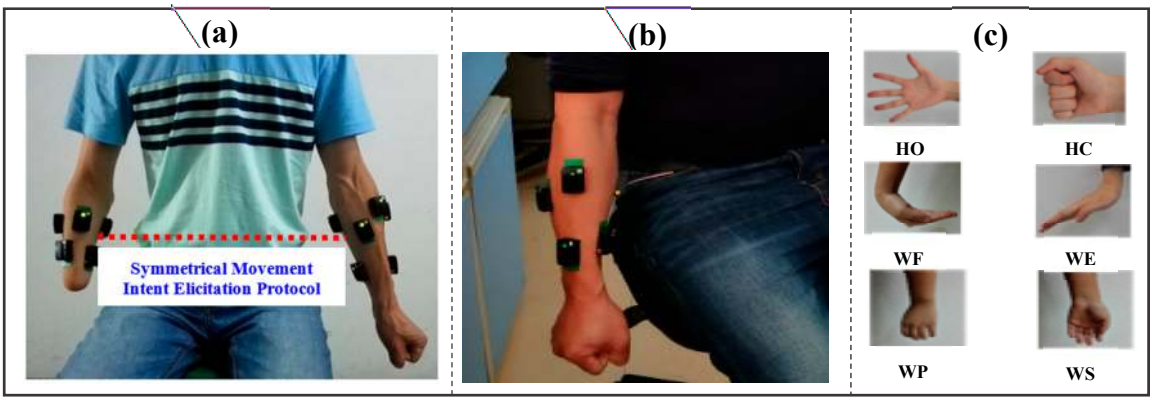

Figure 2. Pre-experimental settings showing the placement of surface EMG electrodes on the residual limb of a representative amputee and healthy subject's limb alongside the active limb movement classes considered in the study. (**a**) Symmetrical placement of the wireless EMG signal sensors on the intact and amputated arm muscles of a representative amputee, (**b**) EMG electrode placement on the forearm of a representative healthy subject, (**c**) The classes of active targeted limb movements considered in the study. Note that: HO, HC, WF, WE, WP, WS, denotes hand open, hand close, wrist flexion, wrist extension, wrist pronation, and wrist supination, respectively.

Following the audio prompt, the subjects were required to perform muscle contractions conforming to the above described classes of targeted arm movements in which each movement was maintained for 5 s. And a rest session of 5 s was introduced between two consecutive classes of active movements to prevent the subjects from having fatigue. Meanwhile, each movement class got repeated five times, leading to 25 s of active EMG signal recordings and 20 s of rest session per experimental trial.

2.3. Preprocessing of the Measure sEMG Data

The sEMG data were obtained during the experimental sessions at a sampling frequency of 1024 Hz, and then stored for further processing. The raw signals were firstly filtered using a 5th-Order Butterworth band pass filter designed with frequency in the range of 20 Hz~500 Hz to enable the extraction of useful components of the signals. Also, power line interferences were eliminated from the filtered signal using 50 Hz notch filter. It should be noted that recorded sEMG signals for all the subjects were preprocessed and analyzed offline using MATLAB version R2017b (Mathworks, Natick, MA, USA) programming tool.

Considering each class of movement, the recorded myoelectric signal is made up of five trials. With a careful observation, the signals were partitioned into contraction/non-contraction segments for each class of targeted movement. To accomplish this task, signals from channels that have clear muscular activities, with respect to the baseline, were visually chosen and combined to obtain an average data stream, which would be needed in the subsequent stage. This process was realized based on the onset and offset times of each muscular activity from a representative channel that is applied to the signals of the other 5 channels.

2.4. Windowing Technique

The EMG data segmentation is one of the important processes used to improve the performance and response time of EMG based pattern recognition control strategy and in this study, overlapping window technique introduced by [13] was adopted to segment the EMG signal into different analysis window. This technique is associated with windowing parameters (length and window increment), where a part of the new analysis window data overlaps with the current window data, and all analysis windows increase with processing time as shown in Figure 3.

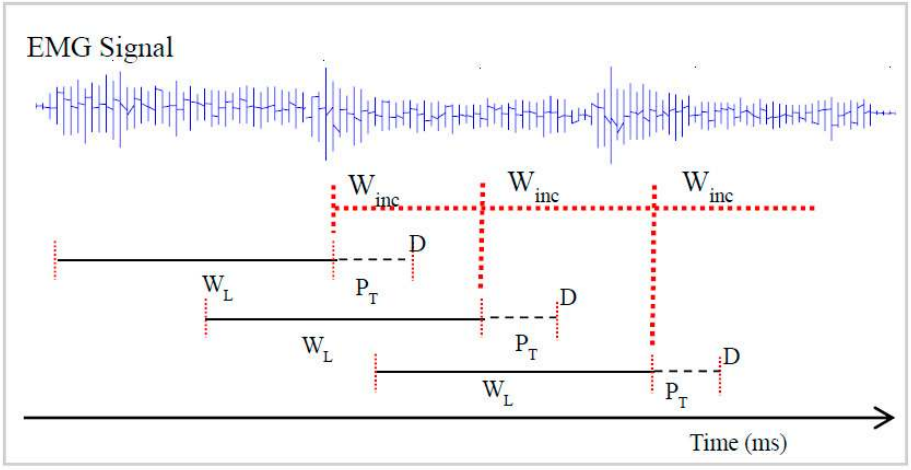

Figure 3. The framework of the overlapping windowing technique for the extraction of feature sets. Note: W_L denotes window length, W_{inc} denotes window increment and P_T represent the processing time.

The processing time is the time require to extract feature sets and the classification algorithm to decode the motion intent. It is worth noting that the window increment is usually shorter than the window length, ideally it is equivalent to the processing time [14]. According to Englehart and

Hudgins [13], a longer window length allows more features to be extracted, resulting in higher classification accuracy, but results in a slower response time of the prosthetic controller, while classification performance reduces with shorter window length but with a faster controller response.

Considering the fact that the utilized windowing parameters would influence the extracted feature characteristics, it is important to determine the optimal windowing parameters that will result in the extraction of accurately robust feature set for multi-class limb movement intent decoding [14,17]. Although, different combinations of windowing parameters have been reported in previous studies with little or no justification in the selection of these parameters. Hence, overlapping analysis window technique with combination of window lengths raging between 100 ms~300 ms and increments from 50 ms–125 ms were examined in this study as shown in Table 1.

Table 1. The combinations of window lengths and increments considered.

S/No.	Window Lengths	Window Increments			
1	100	50	75	-	-
2	150	50	75	100	125
3	200	50	75	100	125
4	250	50	75	100	125
5	300	50	75	100	125

2.5. Feature Extraction Procedure

In this study, a total of sixteen feature extraction methods (including two feature sets proposed previously by our research group) that have been applied for characterizing multi-classes of targeted limb movement intent were selected from four functional EMG feature groups namely: time-domain, frequency-domain, time-series domain, and the statistical features. Furthermore, four feature sets are based on EMG signal amplitude, five are based on nonlinear complexity and frequency information, two are based on time-series modelling, and the remaining five are based on combination of feature sets (Table 2).

Table 2. Time-frequency based features adopted for EMG signal characterization.

Feature Extraction Methods		
S/N	**Features Description**	**Mathematical Expression**
1	Root Mean Square (RMS): It is modeled as amplitude modulated Gaussian random process whose relates to constant force and non-fatiguing contraction [11,26].	$\sqrt{\frac{1}{k}\sum_{n=1}^{k} x_n{}^2}$
2	Waveform Length (WL): This is the aggregate length of the EMG waveform in an analysis window [27,28].	$\sum_{n=1}^{k-1}\left[f\left(\left\|x_{n+1}-x_n\right\|\right)\right]$
3	Mean Absolute Value (MAV): is an average of absolute value of the EMG signal in an analysis time window [12,27].	$\frac{1}{k}\sum_{n=1}^{k}\|x_n\|$
4	Variance (VAR): measures the power of the EMG signal [12,29].	$\frac{1}{N-1}\sum_{k=1}^{N} x^2k$
5	Mean Frequency (MNF): is this feature is calculated as the sum of product of the EMG power spectrum and frequency divided by the total sum of spectrum intensity [27,30].	$\sum_{j=1}^{m} f_j P_j / \sum_{j=1}^{m} P_j$
6	PSR: Power Spectral Ratio(PSR)as ratio between the energy P0 which is nearby the maximum value of the EMG power spectrum and the energy P which is the whole energy of the EMG power spectrum: [31]	$\frac{P_0}{P} : \sum_{j=f0-n}^{f0+n} P_j / \sum_{j=-\infty}^{\infty} P_j$

Table 2. *Cont.*

Feature Extraction Methods		
S/N	**Features Description**	**Mathematical Expression**
7	TTP: Total Power (TTP): computes the total EMG signal power spectrum: [30,32]	$\sum_{j=1}^{M} P_j \ : \ SMO$
8	PKF: Peak Frequency (PKF): this is a frequency at which the maximal power take place [32]	$PKF = \max\left(P_j\right),\ j = 1, \ldots, M$
9	Median Frequency (MDF):is a frequency at which the spectrum is divided into two regions with equal amplitude [27]	$\sum_{j=1}^{MDF} P_j = \sum_{j=MDF}^{M} P_j \ = \frac{1}{2} \ \sum_{j=1}^{M} P_j$
10	4th order Autoregressive Coefficient (AR4): The feature model the signal by previous data point of the EMG signal and as well gives information about the state of muscle contraction [24,27,28].	$\sum_{n=1}^{k} a_n x_{k-i} \ + e_k, a_n = 4$
11	6th order Autoregressive Coefficient (AR6): [11,12,29].	$\sum_{n=1}^{k} a_n x_{k-i} \ + e_k, a_n = 6$
12	TD2: Summation of Square root (ASS) and absolute value of Summation of exponent root and Mean (ASM) of the data in a given analysis window [6]	$ASS \ = \left\lvert\sum_{n=1}^{k} (x_n)^{1/2}\right\rvert, ASM \ = \left\lvert\frac{\sum_{n=1}^{k} (x_n)^{exp}}{k}\right\rvert,$
13	Time Domain Power Spectral Descriptor (TD-PSD): this feature sets estimate a set of power spectrum characteristics directly from the time-domain: [33,34]	$f_1 = \log(m_0),\ f_2 = \log(m_0 - m_2)$ $f_3 = \log(m_0 - m_4), f_5 = \ \frac{m_2}{\sqrt{m_0 m_4}}, f_6 = \log\left(\frac{\sum_{j=0}^{N-1} \lvert\Delta x\rvert}{\sum_{j=0}^{N-1} \lvert\Delta^2 x\rvert}\right)$
14	Four time Domain and AR6 (TDAR6): Combination of RMS and AR6 [23,24,26,27]	*RMS* and AR6
15	Five time Domain and AR6 (TD5AR6): combination of MAV, RMS, WL, ZC, SSC and AR6(ZC: Zero Crossing, SSC: Slope Sign Change) [11,12,26–29,35]	MAV, *RMS*, *WL*, *ZC*, *SSC*, *AR6* $ZC = \sum_{n=2}^{k-1} [f(x_n - x_{n-1}) * (x_n - x_{n+1})]$ $SSC = \sum_{n=1}^{k-1} [sgn(x_n * x_{n+1}) \cap (x_n - x_{n+1}) \geq \text{Thr.}]$
16	Novel Time Domain Feature Set (NTDFS), that combined neuromuscular information for adequate characterization of EMG signal patterns even in the presence of co-founding factors [36]	$SISx_n = \ \sum_{n=0}^{N-1} x[n]^2,\ normRSdx_1 =$ $\frac{1}{N} \ \sum_{n=0}^{N-1} dx_1[n]^2, normRSDx_2 =$ $\frac{1}{N} \ \sum_{n=0}^{N-1} dx_2[n]^2, normLogDet. =$ $norm(e^{\frac{1}{N} \sum_{n=0}^{N-1} \log(x[n])}),\ mMSR, and\ mASM$

It should be noted that features from the above described categories were considered to adequately account for all possible types of meaningful information associated with EMG signal classification [5]. Meanwhile, the accuracy, computational complexity, and robustness of the feature extraction methods were systematically investigated for each combination of window length and increment presented in Table 1 using a number of evaluation metrics described in the Section 2.6.

2.6. Evaluation Metrics

To effectively evaluate the performance of the feature extraction methods, in terms of characterizing multiple-classes of movement intents in the context of EMG-PR system, four different metrics were utilized which are described as follows.

1. The commonly applied metric know as classification error (CE) which represent the number of non-correctly identified samples over the sum of all samples (Equation (1)) was utilized to evaluate the classification accuracy of the feature extracted methods:

$$\textbf{CE} = \frac{\textbf{Number of incorrectly classified samples}}{\textbf{Total number of testing samples}} * 100 \quad (1)$$

2. The F1_score was utilized to further validate the performance of the extracted feature sets. This metric was computed as the weighted average of precision and recall (Equations (2) and (3)) [37]. Basically, the F1_score reveals the performance of the classifier in classifying the data points of a particular feature set compared to others,

$$\textbf{Precision} = \frac{TP}{TP + FP} \ , \ \textbf{Recall} = \frac{TP}{TP + FN} \tag{2}$$

$$\textbf{F1}_{\textbf{score}} = \frac{2 * \textbf{Recall} * \textbf{Precision}}{\textbf{Recall} + \textbf{Precision}} \tag{3}$$

where TP is the count of true positives, TN is the count of true negatives, FP represent number of false positives, and FN is the number of false negatives obtained from a confusion matrix. It is worth noting that F1_score reaches its best value at 1 and worst at 0.

3. In principle, the computation time of a feature set would generally influence the response time of the microprocessor-based controller embedded in the prosthesis socket [15]. In this regard, the computation time of each extracted feature set presented in Table 2 was investigated by adopting the formulae in Equation (4) that was proposed by Weir and Farell [15],

$$D = \frac{1}{2}W_L + \frac{1}{2}W_{inc} + P_T \tag{4}$$

where D is the delay, W_L is the window length, W_{inc} is the window increment and P_T is the signal processing time. It should be noted that the configuration of the system utilized for this study is Microsoft window 7 professional with 64-bit operating system, Intel(R) Core(TM) i7 processor with processing speed of 3.6 GHz and 8 GB random access memory.

4. In the context of EMG-based pattern recognition system, an ideal feature extraction method would normally be influenced/affected by unwanted disturbances that may degrade the decoding of the user's intended limb movement. Therefore, it is important to quantify the robustness of a feature in other to guarantee that the features would be consistently stable when applied in real-life applications. In this regard, the stability index (S_{Index}) metrics adopted in a previous study [38], which is defined by Equation (5) was applied to examine the robustness of the feature extraction methods in the presence of noise,

$$S_{Index} = \frac{\frac{1}{N}\sum_{i=1}^{N} CA_i}{\left[\frac{1}{N-1}\sum_{i=1}^{N}\left(CA_i - \frac{1}{N}\sum_{i=1}^{N} CA_i\right)^2\right]^{\frac{\propto}{2}}} \tag{5}$$

where the numerator is the average classification performance, the denominator is the scaled standard deviation, $\propto$ is the scaled value and is set to 0.1 and N is the sample size. The value of $\propto$ was chosen after many trials.

2.7. Machine Learning Classification Technique

To decode the subjects' limb movement intent from the constructed feature matrix, two machine learning based classification algorithms including support vector machine (SVM) and linear discriminant analysis (LDA) were utilized. Meanwhile, five-fold cross validation technique was employed for the partitioning of the extracted feature matrix into training and testing sets. The rationale behind considering these classification schemes is that their performances are relatively good, especially when considering multi-class problems [1,10,36]. Therefore, we built an SVM classifiers driven by radial basis function, and compared its classification performance with that of the LDA classifiers. Notably, we found that SVM achieved an overall accuracy that is slightly lower in comparison to the LDA. Meanwhile, the LDA classification scheme runs much faster than its SVM counterpart. Also due

to its relatively simple structure, and easy implemented in real-time, it was adopted in the current study [6,8,10].

3. Results

3.1. Analysis of the Feature Sets Based on Classification Error across Windowing Parameters

In this section, the properties of the different extracted feature sets were studied in terms of their classification error (CE) across combinations of window lengths and increments (Table 1) for movement intent decoding based on the LDA algorithm. The obtained results across subjects and movement classes is presented using the Heatmap plot shown in Figure 4. This analysis shows the average CE across subjects (amputees and able-bodied subjects) and movement classes, where the columns represent the different extracted features and the rows denote the combinations of windowing parameters utilized in this study.

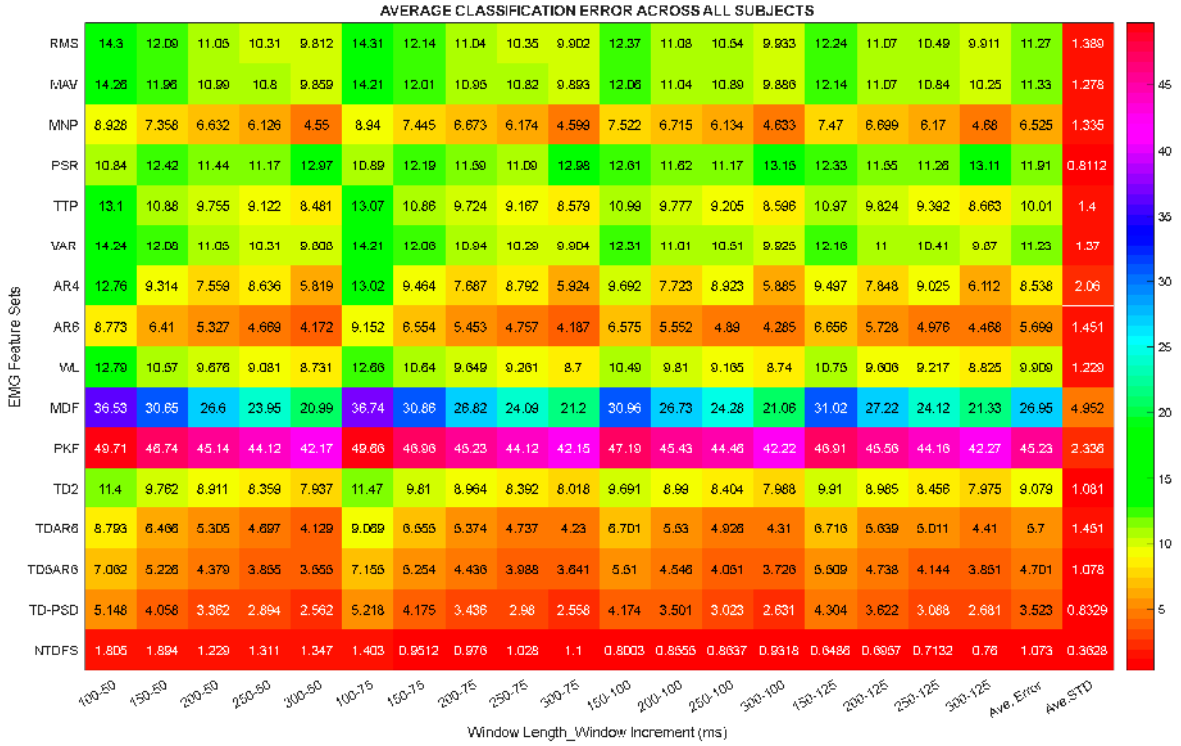

Figure 4. Heatmap plot of classification error across combinations of window lengths and increments.

It is worth noting that preliminary analysis showed that the symmetrical movement intent elicitation experiment protocol (Figure 2a) adopted in this study was helpful in aiding the amputee subjects perform seven of the pre-defined classes of movements with their amputated limbs. Meanwhile, all the results presented in this study are based on the recordings from the amputated limb, and not both limbs.

From Figure 4, it could be observed that the PKF and MDF features achieved the lowest classification performances with an average CE value of 45.23 ± 4.95% and 26.95 ± 2.33% while the NTDFS, TD-PSD, and TD5AR6 recorded an average CE of 1.07 ± 0.35%, 3.52 ± 0.83%, and 4.70 ± 1.08%, respectively, which were much better than the other feature extracted methods.

In summary, by critically analyzing the results shown in Figure 4, it was found that keeping the window length constant and varying the increment parameter does not meaningfully influence the classification performance of the extracted feature sets. On the other hand, varying the window length with a relatively constant increment would have more influence on the classification performance of the extracted feature sets. For instance, considering the RMS feature, when the increment parameter

is fixed at 50ms, average decoding errors of 14.05%, 12.34%, 11.46%, and 10.35% were recorded for 150 ms, 200 ms, 250 ms, and 300 ms window lengths, respectively. Meanwhile, when the window length was kept constant at 200 ms, average decoding errors of 11.46%, 11.50%, 11.60%, 11.55% were obtained for 50 ms, 75 ms, 100 ms, and 125 ms increments, respectively. Overall it could be deduced that most features achieved the least CE at window increment of 100 ms, hence the subsequent analysis were conducted using a window increment of 100 ms.

3.2. Analysis of the Feature Sets Based on Computation Time across Windowing Parameters

In this section, the characteristics of the feature sets were further studied based on their computation time (CT) across different combination of window lengths and increments, and the analysis was done based on sEMG data from both category of subjects, as shown in the Heatmap plot presented in Figure 5. The columns represent all the considered features extraction methods while the rows depicts the different combination of window lengths and window increments.

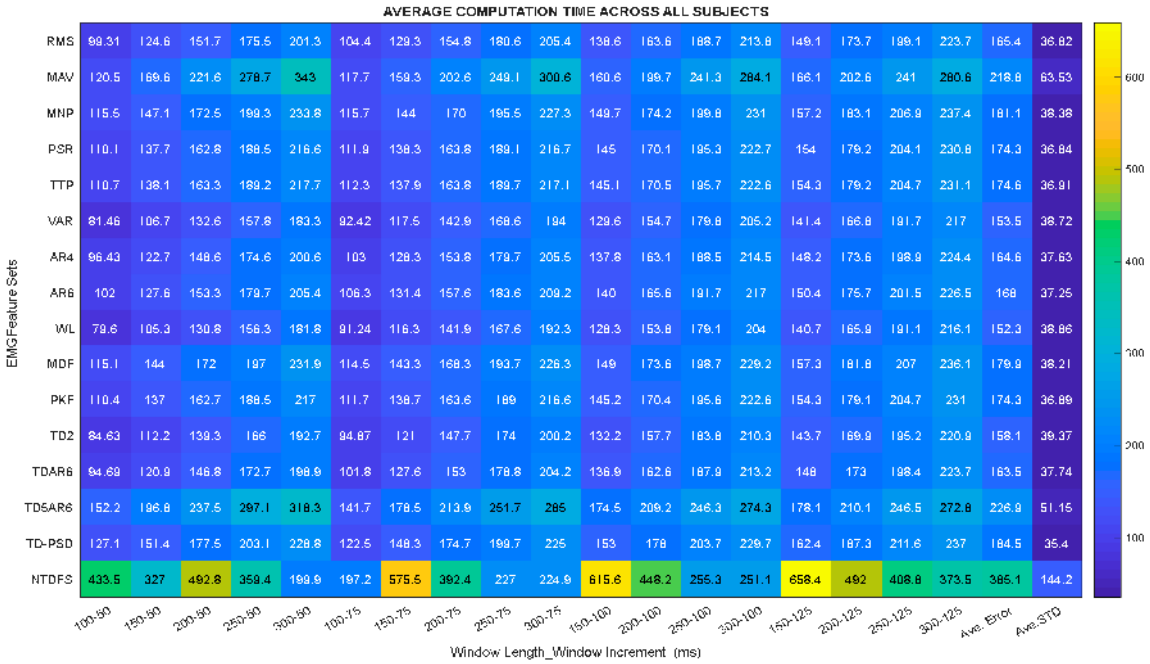

Figure 5. Heatmap plot of Computation time across combinations of window lengths and increments.

By closely analyzing the CT of each feature extraction method across different combinations of window lengths and increments (Figure 5), it could be seen that WL and TD2 features achieved the smallest CT of approximately 152.3 ms and 158.1 ms, while NTDFS and TD5AR6 features recorded relatively higher average CT of 385.1 ms and 226.9 ms, respectively. One possible explanation for the high computation time recorded by the NTDFS and TD5AR6 descriptors may be because they both consist of a combination of features, thus, leading to a correspondingly higher dimension compared to the other feature extraction methods.

Fundamentally, the higher the dimension of the extracted feature set, the more the computation time. In summary, it was observed that the smaller the difference between the window length and increment, the lesser the computation time, which would lead to the realization of a prosthesis controller with relatively faster response time. On the contrary, the larger the difference between the window length and its increment, the more the computation time, leading to a prosthesis controller with slower response time although it would result in higher classification performance. Hence, such tradeoff could be taking into consideration by prostheses manufacturers. Importantly, this phenomenon has rarely been reported till date and this phenomenon could be observed with the other feature extraction methods investigated in this study.

3.3. Analysis of the Feature Sets' Data Point Characterization Using F1-Score Metric

In this section, the performance of the feature sets in terms of data point characterization were also examined by computing the F1-score values for both the amputees and able-bodied subjects across all the movement classes and the obtained results are presented in Tables 3 and 4 as follows using window length ranging from 150 to 300 ms with 100 ms increment. It could be seen from the results presented in Table 3 that the NTDFS, TD-PSD, and TD5AR6 features achieved relatively high F1-scores of approximately 0.99 ± 0.003%, 0.97 ± 0.005%, and 0.96 ± 0.005%, respectively, as against the PKF and MDF features that recorded the lowest accuracy of 0.58 ± 0.03%, and 0.72 ± 0.04%, across subjects.

Table 3. Average motion classification accuracies based on F1_score metric for able-bodied subject.

S/No.	Window Length → / Feature Sets ↓	150	200	250	300	Mean ± SD
1	RMS	0.8829	0.8978	0.9046	0.9096	0.8987 ± 0.0116
2	MAV	0.8862	0.8978	0.9039	0.9103	0.8995 ± 0.0103
3	MNP	0.9167	0.9269	0.9343	0.9392	0.9293 ± 0.0098
4	PSR	0.8750	0.8843	0.8877	0.8647	0.8779 ± 0.0103
5	TTP	0.8955	0.9089	0.9157	0.9228	0.9107 ± 0.0116
6	VAR	0.8837	0.8985	0.9039	0.9099	0.8990 ± 0.0112
7	AR4	0.8813	0.9086	0.9204	0.9324	0.9107 ± 0.0219
8	AR6	0.9253	0.9387	0.9477	0.9550	0.9417 ± 0.0128
9	WL	0.9053	0.9131	0.9204	0.9242	0.9157 ± 0.0084
10	MDF	0.6654	0.7083	0.7384	0.7759	0.7220 ± 0.0468
11	PKF	0.4987	0.5109	0.5223	0.5376	0.5174 ± 0.0165
12	TD2	0.9014	0.9093	0.9171	0.9220	0.9124 ± 0.0090
13	TDAR6	0.9229	0.9394	0.9456	0.9546	0.9406 ± 0.0133
14	TD5AR6	0.9390	0.9517	0.9586	0.9619	0.9528 ± 0.0101
15	TD-PSD	0.9559	0.9657	0.9714	0.9753	0.9671 ± 0.0084
16	NTDFS	0.9904	0.9934	0.9952	0.9964	0.9938 ± 0.0026

Table 4. Average motion classification accuracies based on F1_score metric for amputee subject.

S/No.	Window Length → / Feature Sets ↓	150	200	250	300	Mean ± SD
1	RMS	0.8816	0.8912	0.8948	0.9014	0.8922 ± 0.0083
2	MAV	0.8852	0.8931	0.8979	0.9034	0.8949 ± 0.0077
3	MNP	0.9366	0.9422	0.9461	0.9497	0.9436 ± 0.0056
4	PSR	0.8761	0.8870	0.8919	0.8755	0.8826 ± 0.0081
5	TTP	0.8958	0.9057	0.9097	0.9143	0.9064 ± 0.0079
6	VAR	0.8819	0.8919	0.8960	0.9013	0.8928 ± 0.0082
7	AR4	0.9262	0.9384	0.9458	0.9514	0.9405 ± 0.0109
8	AR6	0.9065	0.9198	0.9287	0.9346	0.9224 ± 0.0122
9	WL	0.9100	0.9100	0.9200	0.9200	0.9150 ± 0.0058
10	MDF	0.6703	0.7199	0.7415	0.7671	0.7247 ± 0.0411
11	PKF	0.5495	0.5743	0.5835	0.6141	0.5804 ± 0.0267
12	TD2	0.9123	0.9184	0.9221	0.9256	0.9196 ± 0.0057
13	TDAR6	0.9449	0.9517	0.9559	0.9604	0.9532 ± 0.0066
14	TD5AR6	0.9516	0.9583	0.9612	0.9643	0.9589 ± 0.0054
15	TD-PSD	0.9622	0.9656	0.9694	0.9730	0.9676 ± 0.0047
16	NTDFS	0.9830	0.9863	0.9877	0.9895	0.9866 ± 0.0028

Also for the amputee subjects, similar trend was observed regarding the features performance with no significant differences across the varying window lengths. Taking a closer look at the F1-score results for both the able-bodied subjects and amputees, it could be seen that the abled-bodied subjects recorded relatively higher values, basically because the amputees had limited residual muscle and

could not provide sufficient EMG information for accurate decoding of their targeted limb movement intents. This phenomenon has also been verified by a number of previous studies [14,16]. Overall, the characteristics of the feature extraction methods based on the F1-score metric is also found to be consistent with the previous two metrics, which further confirms the validity of our findings, thus far.

3.4. Effect of Disturbance on the Feature Set Performance

The robustness of the individual feature extraction methods were examined by introducing specific amount of random noise into the sEMG signals and then using each of the selected feature extraction methods to characterize the participants' limb movement intents. Thus, a statistically driven stability index ($S_{\_Index}$) metric defined in Section 2.6 (Equation (5)) was utilized to evaluate the robustness of the feature sets considered and the obtained results for the able-bodied and amputee subjects were presented in Figures 6 and 7 respectively.

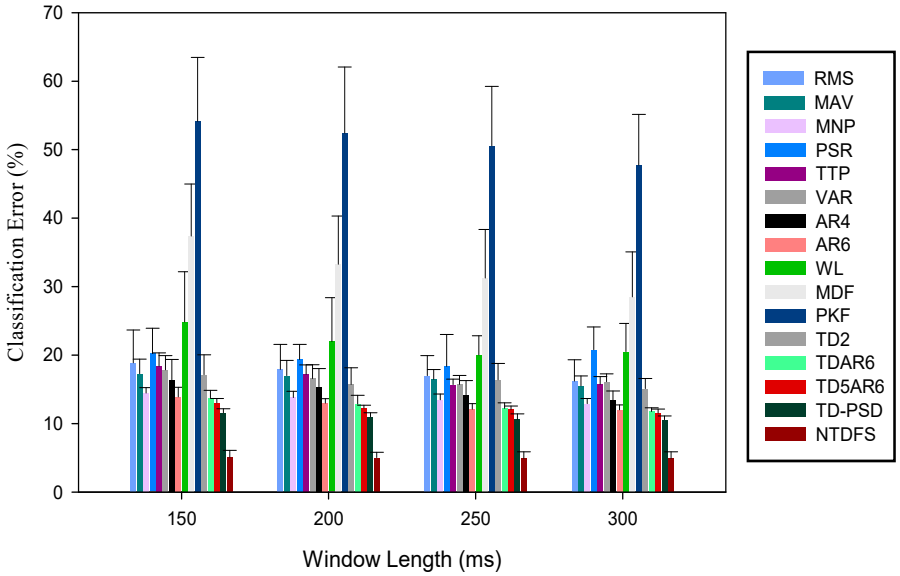

Figure 6. Mean classification error of the features in terms of their robustness to external noise across varying window length at window increment of 100 ms for abled-bodied subjects.

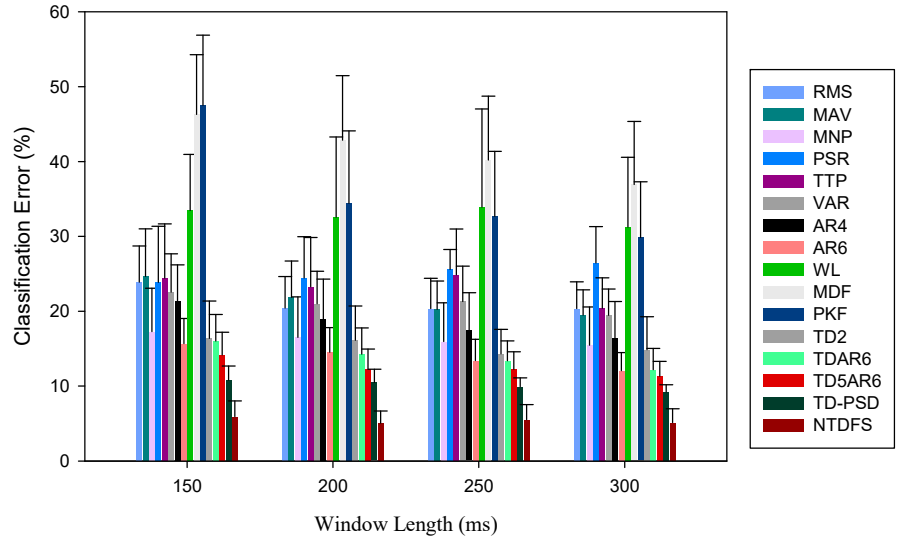

Figure 7. Mean classification error of the features in terms of their robustness to external NOISE across varying window length at window increment of 100 ms for amputee subjects.

From the result illustrated in Figures 6 and 7, it could be seen that the CE of the feature sets decreased with increase in window length, which is consistent with previous results. Furthermore, the results show that multi-features are more robust to disturbance compared to single features. As the noise was introduced, NTDFS feature recorded the least CE values ranging between 4.19%~5.94% for both able-bodied and amputee subjects, correspondingly across window lengths (150 ms~300 ms) compared to other feature sets. Meanwhile, the PKF and MDF are mostly affected by the noise, thus recording CE between 47.51%~54.14%, and 46.30%~37.41%, respectively, indicating high-level of instability in the presence of noise.

Additionally, the standard error bars in Figure 6 were observed to be relatively lower than those in Figure 7 across subjects and window lengths, thus, indicating that the able-bodied subjects' data resulted in a better $S_{\_Index}$ compared to the amputee subjects. In other words, the amputee subjects are more susceptible to the disturbance compared to the able-bodied subjects. Since the amputee subjects are the end-user of the myoelectric device, there is a need to employ a robust feature sets that could enhance movement intent decoding task needed for the EMG-PR control system regardless of the windowing parameters adopted.

3.5. The Effect of Number of Channels on the Feature Sets across Windowing Parameters

Finally, we investigated the influence of the number of electrode channels on limb movement intent classification across window length (150 ms~300 ms) with a window increment of 100 ms for all the feature sets using sEMG recordings from 2, 4, and 6 channels, and the obtained results are presented in Figure 8a–f for both the able-bodied and amputee subjects. Figure 8a,b represent the classification performances of all the features using two channels. Therefore, the CE of all the feature sets (except PKF) decreased with increasing window length and this trend was consistent with the other results obtained when sEMG recordings from 4 and 6 channels were utilized (Figure 8c–f) for both able-bodied and amputee subjects. In other word, the CE reduces with increasing window length and number of channels regardless of the kind of feature set employed.

In like manner, the classification performances of the feature extraction methods were again observed to be better for the able-bodied subjects compared to the amputee subjects (Figure 8a–f) when sEMG recordings from the same number of electrode channels were utilized. In other words, it could be seen that the PKF (able-bodied: 65.65 ± 1.58%, amputee: 72.90 ± 0.72%) and MDF (able-bodied: 52.65 ± 3.02%, amputee: 56.21 ± 3.21%) features recorded the highest CE values for 2-channel sEMG recordings regardless of the type of participants, while the NTDF (able-bodied: 4.05 ± 0.83%, amputee: 6.15 ± 1.54%) and TD-PSD (able-bodied: 16.54 ± 1.78%, amputee: 22.81 ± 2.55%) features achieved the least CE values.

In similar trend, the same phenomenon was observed for 4-channels and 6-channels sEMG recording though with slight decrease in CE values. In general, utilizing sEMG recordings from 6-channels achieved the lowest CE for all the feature sets. Hence, such variability indicate that the number channels utilized may influence the classification performance of EMG-PR classifiers. It is important to note that the computation time of all the features across varying window length increases with increasing number of electrode channels, indicating a trade-off between number of electrode channels and computation time.

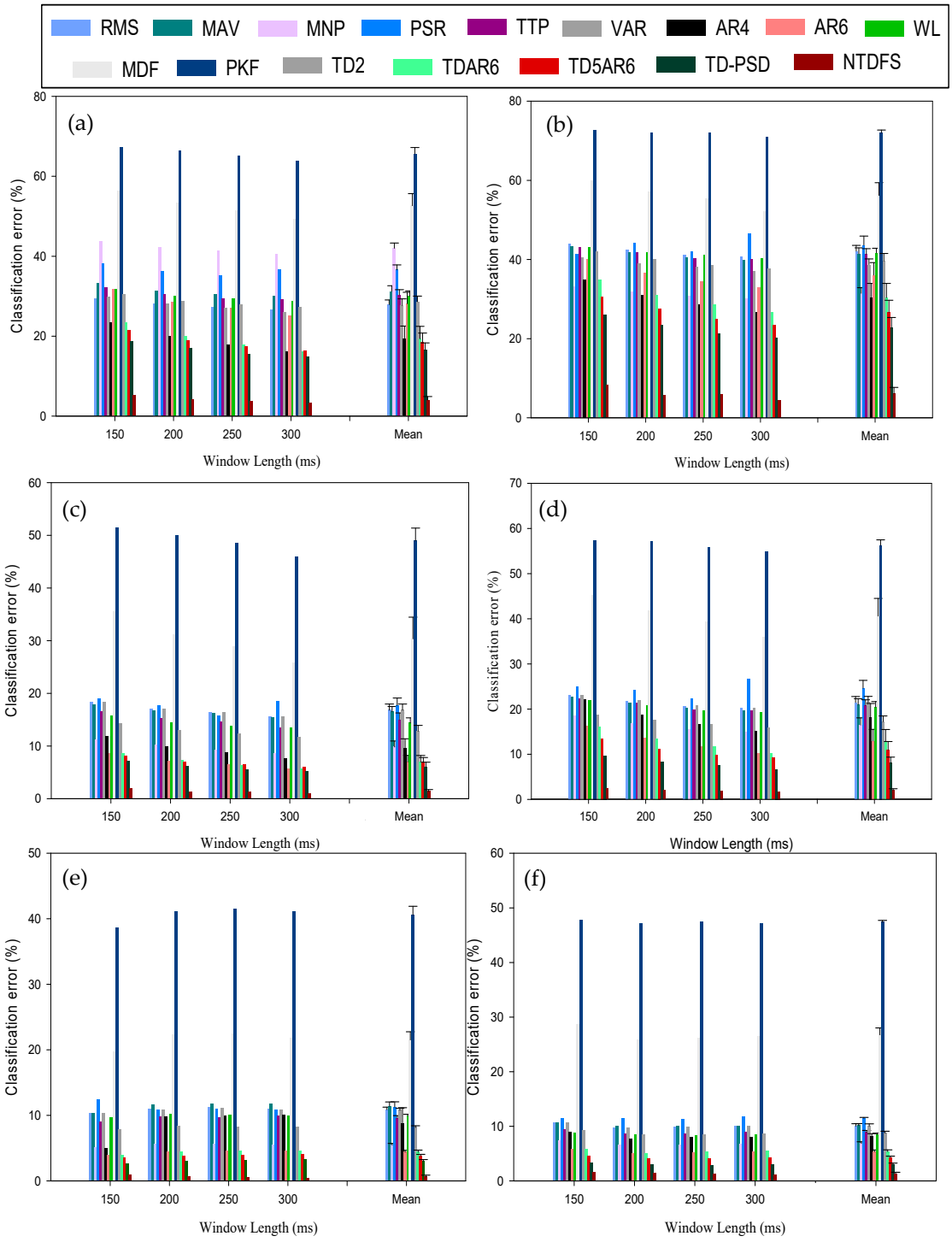

Figure 8. Mean classification error across varying window length at window increment of 100 ms for (**a**) 2-channel recording of able-bodied subjects; (**b**) 2-channel recording of amputee subjects (**c**) 4-channel recording of able-bodied subjects; (**d**) 4-channel recording of amputee subjects (**e**) 6-channel recording of able-bodied subjects (**f**) 6-channel recording of amputee subjects.

4. Discussion

A detailed analysis of the experimental results obtained from this study revealed that multiple factors, including windowing parameters, choice of feature sets, and number of electrode channels would influence the overall performance of myoelectric pattern recognition system that adopts linear

discriminant analysis classifier. A few previous works recognized the need for such study and they had attempted to investigate the effect of window length and increment on myoelectric controller delay though in the context of limited factors [12–14,16,38]. Remarkably, this study considered additional critical factors by investigating the effect and interactions amongst windowing parameters and feature sets with respect to classification error, computational time, robustness to noise and number of electrode channels on the overall performance of pattern recognition system. Investigation on the interaction of these factors towards realizing a consistently stable and accurate EMG-PR scheme for multi-class movement intent decoding has rarely been considered till date. It is worth noting that this investigation may be adopted in other fields of study [39,40].

More precisely, the results presented in Figure 4 demonstrate the effect of windowing parameters (window length and window increment) on the sixteen feature sets and their resultant influence on the classification performance of the EMG-PR classifier across movement classes and subjects. In general, for all the considered feature sets, the classification error reduces as the window length increases, however we found that window increment do not have direct effect on the classification performance which corroborate the findings from a previous study [14]. Additionally, the multi-feature sets of NTDFS, TD-PSD, and TD5AR6 achieved the minimum average classification errors and deviations of 1.07 ± 0.36%, 3.52 ± 0.83%, and 4.70 ± 1.07%, across subjects compared to the single features selected from the four EMG feature functional groups presented in Table 2. One possible reason for the improved performance observed for the multiple feature sets of NTDFS, TD-PSD, and TD5AR6 should be because they integrate neuromuscular information from multiple dimensions, thereby aggregating rich set of information for the movement intent decoding tasks compared to the other single features. From the perspective of the single feature set, AR6 and MNP were observed to have achieved better performance than other single features by recording classification error as low as 5.70 ± 1.45%, and 6.52 ± 1.33%, respectively. One core benefit of this findings is that the classification performance of EMG-PR system can be improved by using a combination of features from the four EMG feature functional groups presented in Table 2, rather than considering single feature set. Therefore, this findings corroborates the report of a previous study [39].

Generally, the least classification error across features was achieved at window length of 300 ms and increment of 100 ms and it could be seen that window increment do not have direct influence on the classification performance. Most features recorded the least classification error at window increment of 100 ms hence it was adopted for subsequent results presented in this study. Analysis of computation time of the feature sets across varying window length and increments was also reported in Figure 5. Here, we observed from the result that the multi-features attracts high computation time, compared to the single features. From the angle of computational complexity, the multiple NTDFS feature set that recorded the lowest movement intent decoding error was observed to have had the highest average computation time (385.1 ms) followed by the TD5AR6 multiple feature (226.9 ms). In addition, increasing the analysis window length resulted to corresponding increase in computation time, indicating a trade-off between classification performance and computation time. Therefore, this further provided us with the insight that it may be beneficial to consider features with relatively lower classification error and slightly higher computation time if the goal is to achieve a classifier with high performance in terms of accuracy that could also output its decision within a reasonable time-frame.

The performances of the feature sets were examined across varying window length of 150 ms–300 ms at a window increment 100 ms based on the feature data points in the feature space using F1-score metric, and the outcome was presented in Tables 3 and 4 for both able-bodied and amputee subjects. From detailed analysis based on EMG recordings from both categories of subjects (amputees and able-bodied individuals), it was observed that the NTDFS and TD-PSD (multiple features) recorded the highest accuracies as against the PKF and MDF (single features) that recorded the lowest accuracies. Also, Tables 3 and 4 showed that there is no significant difference in the classification accuracy across the varying window length, while the F1-score results were consistent with the results presented in Figure 1, thereby further supporting our findings.

Furthermore, we investigated the performances of the feature sets in the presence of a disturbance, by introducing random noise into the EMG recording signal and the features' performances were evaluated using the stability index metric across subjects and window lengths (150 ms–300 ms) as shown in Figures 6 and 7. In this investigation, we found that the multi features, such as NTDFS, TD-PSD, and TD5AR6 recorded the least classification error, while PKF, MDF, and WL features recorded the highest classification error for both able-bodied and amputee subjects. Interestingly, this result further proves that multi features would be more robust to external interferences (noise) compared to the single features irrespective of the windowing parameters considered. Also, we observed that the effect of the introduced noise was much obvious on the sEMG recordings of the amputees compared to the able-bodied, which could be attributed to the fact that the residual arm muscles of the amputees may produce less-rich information than those of the able-bodied subjects in an ideal situation. Therefore, considering the fact that amputees are the end-users of the myoelectric device, there is need to employ a robust feature sets that will help to enhance classification performance of EMG-PR control system regardless of the windowing parameters adopted.

Lastly, we examined the effect of the number of channels on the extracted features across varying window parameters and we found that the classification error of the features reduces with increasing number of channels for both able-bodied and amputee subjects. (Figure 8a–f). In similar trends with other results, the multi-features outperformed the single features when 2-channels, 4-channels and 6-channels were considered. Finally, by critically analyzing of our results, we discovered that when classification error, computation time, and number of electrodes were considered together, most feature sets achieved good classification performance with optimal windowing parameters of 250 ms/100 ms. Also, discoveries from this study through the systematic approach adopted can facilitate positive development in other areas where optimal features and machine learning driven approaches are required [41–50]. Last, one limitation of the current work is that the EMG pattern recognition system for movement intent decoding was analyzed in an off-line mode, and we hope to conduct online and real-time analysis in our future work. By doing so, it would further broaden the applicability of the current study in real-life applications.

5. Conclusions

In developing intelligent multifunctional prostheses where symmetrical limb motion intent elicitation protocol was adopted, this study systematically investigated the characteristics of a range of features across varying windowing parameters when applied for movement intent decoding in the context of pattern recognition system,. The interrelation and impact of different windowing parameters on the performances of the feature sets were extensively explored with respect to accuracy, computation complexity, robustness to additive random noise and number of electrode channels. From the experimental results, we found that a combination of features mostly achieved high classification performance with correspondingly higher computation time compared with their individual counterparts (single features) that had lower computation time and high classification error. Interestingly, this phenomenon explains the trade-off that exist between accuracy and controller delay in the practical use of upper limb prosthesis in real-life applications. Furthermore, we discovered that the combinations of features are more robust to noise, compared to single features, and with lesser channels they can still achieved relative good classification performance across varying windowing parameters regardless of the subject category. Particularly, NTDFS, TD-PSD, and TD5AR6 features exhibited consistent stability, robustness, and accuracy across all the windowing parameters for both, able-bodied and amputee subjects compared to the other features. Findings from this study would provide researchers and engineers with a framework for proper selection of appropriate feature set, windowing parameters, and signal conditioning, required to develop a computationally efficient PR-based control strategy for intelligently smart prostheses and other PR based systems aimed at providing smart health care services.

Author Contributions: Conceptualization, M.G.A., and O.W.S., investigation, M.G.A., and O.W.S., methodology, M.G.A. and O.W.S.; software, M.G.A.; validation, M.G.A.; subjects recruitment, L.W.; data collection, O.W.S., Y.G., and Y.J. data analysis, M.G.A., and O.W.S.; data interpretation, M.G.A., and O.W.S.; writing—original draft preparation, M.G.A.; writing—review and editing, O.W.S., S.C., P.F., A.K.S., and G.L.; supervision, G.L.; funding acquisition, G.L. All authors have read and agreed to the published version of the manuscript.

Funding: The research work was supported in part by the National Natural Science Foundation of China under Grants (#U1613222, #81850410557, #U1913601, #8201101443, #5061773364), CAS President's International Fellowship Initiative Grant (#2019PB0036), Shenzhen Science and Technology Program (#SGLH20180625142402055), the Shenzhen Governmental Basic Research Grant (#JCYJ20160331185848286), the International Collaboration Program, Natural Science Foundation of Guangdong Province (2019A050510029), the Natural Science Foundation of Guangdong Province (2018A030313065), the Science, Technology and Innovation Commission of Shenzhen Municipality Fund (JCYJ20170818163445670), and the Shenzhen Institute of Artificial Intelligence and Robotics for Society.

Acknowledgments: Mojisola G. Asogbon Samuel sincerely appreciate the support of the Chinese Government Scholarship (CSC) in the pursuit of a Ph.D. degree at the University of Chinese Academy of Sciences, Beijing, China.

Conflicts of Interest: The authors declare no conflict of interest.

References

1. Samuel, O.W.; Asogbon, M.G.; Geng, Y.; Al-Timemy, A.H.; Pirbhulal, S.; Ji, N.; Chen, S.; Fang, P.; Li, G. Intelligent EMG pattern recognition control method for upper-limb multifunctional prostheses: Advances, current challenges, and future prospects. *IEEE Access* **2019**, *7*, 10150–10165. [CrossRef]
2. Geng, Y.; Ouyang, Y.; Samuel, O.W.; Chen, S.; Lu, X.; Lin, C.; Li, G. A robust sparse representation based pattern recognition approach for myoelectric control. *IEEE Access* **2018**, *6*, 38326–38335. [CrossRef]
3. Khokhlova, M.; Migniot, C.; Morozov, A.; Sushkova, O.; Dipanda, A. Normal and pathological gait classification LSTM model. *Artif. Intell. Med.* **2019**, *94*, 54–66. [CrossRef] [PubMed]
4. Amsüss, S.; Goebel, P.M.; Jiang, N.; Graimann, B.; Paredes, L.; Farina, D. Self-correcting pattern recognition system of surface EMG signals for upper limb prosthesis control. *IEEE Trans. Biomed. Eng.* **2014**, *61*, 1167–1176. [CrossRef] [PubMed]
5. Phinyomark, A.; Khushaba, R.N.; Scheme, E. Feature extraction and selection for myoelectric control based on wearable EMG sensors. *Sensors* **2018**, *18*, 1615. [CrossRef] [PubMed]
6. Samuel, O.W.; Zhou, H.; Li, X.; Wang, H.; Zhang, H.; Sangaiah, A.K.; Li, G. Pattern recognition of electromyography signals based on novel time domain features for amputees' limb motion classification. *Comput. Electr. Eng.* **2018**, *67*, 646–655. [CrossRef]
7. Bi, M. Control of Robot Arm Motion Using Trapezoid Fuzzy Two-Degree-of-Freedom PID Algorithm. *Symmetry* **2020**, *12*, 665. [CrossRef]
8. Samuel, O.W.; Fang, P.; Chen, S.; Geng, Y.; Li, G. Activity recognition based on pattern recognition of myoelectric signals for rehabilitation. In *Handbook of Large-Scale Distributed Computing in Smart Healthcare*; Springer: Cham, Switzerland, 2017; pp. 427–442.
9. Rohm, M.; Schneiders, M.; Müller, C.; Kreilinger, A.; Kaiser, V.; Müller-Putz, G.R.; Rupp, R. Hybrid brain–computer interfaces and hybrid neuroprostheses for restoration of upper limb functions in individuals with high-level spinal cord injury. *Artif. Intell. Med.* **2013**, *59*, 133–142. [CrossRef]
10. Moloudi, M.; Mazinan, A.H. Controlling disturbances of islanding in a gas power plant via fuzzy-based neural network approach with a focus on load-shedding system. *Complex Intell. Syst.* **2019**, *5*, 79–89. [CrossRef]
11. Samuel, O.W.; Li, X.; Geng, Y.; Asogbon, M.G.; Fang, P.; Huang, Z.; Li, G. Resolving the adverse impact of mobility on myoelectric pattern recognition in upper-limb multifunctional prostheses. *Comput. Biol. Med.* **2017**, *90*, 76–87. [CrossRef]
12. Zardoshti-Kermani, M.; Wheeler, B.C.; Badie, K.; Hashemi, R.M. EMG feature evaluation for movement control of upper extremity prostheses. *IEEE Trans. Rehabil. Eng.* **1995**, *3*, 324–333. [CrossRef]
13. Englehart, K.; Hudgins, B. A robust, real-time control scheme for multifunction myoelectric control. *IEEE Trans. Biomed. Eng.* **2003**, *50*, 848–854. [CrossRef] [PubMed]
14. Smith, L.H.; Hargrove, L.J.; Lock, B.A.; Kuiken, T.A. Determining the optimal window length for pattern recognition-based myoelectric control: Balancing the competing effects of classification error and controller delay. *IEEE Trans. Neural Syst. Rehabil. Eng.* **2011**, *19*, 186–192. [CrossRef] [PubMed]

15. Li, G.; Schultz, A.E.; Kuiken, T.A. Quantifying pattern recognition based myoelectric control of multifunctional transradial prostheses. *IEEE Trans. Neural Syst. Rehabil. Eng.* **2010**, *18*, 185–192. [PubMed]
16. Menon, R.; Di, C.G.; Lakany, H.; Petropoulakis, L.; Conway, B.A.; Soraghan, J.J. Study on interaction between temporal and spatial information in classification of EMG signals for myoelectric prostheses. *IEEE Trans. Neural Syst. Rehabil. Eng.* **2011**, *25*, 1832–1842. [CrossRef] [PubMed]
17. Farrell, T.R. Analysis window induced controller delay for multifunctional prostheses. *Invol. Myoelectric Controls Symp.* **2008**, *2008*, 225–228.
18. Farrell, T.R.; Weir, R.F. The optimal controller delay for myoelectric prostheses. *IEEE Trans. Neural Syst. Rehabil. Eng.* **2007**, *15*, 111–118. [CrossRef]
19. Graupe, D.; Salahi, J.; Kohn, K.H. Multifunctional prosthesis and orthosis control via microcomputer identification of temporal pattern differences in single-site myoelectric signals. *J. Biomed. Eng.* **1982**, *4*, 17–22. [CrossRef]
20. Graupe, D.; Salahi, J.; Zhang, D. Stochastic analysis of myoelectric temporal signatures for multifunctional single-site activation of prostheses and orthoses. *J. Biomed. Eng.* **1985**, *7*, 18–29. [CrossRef]
21. Hefftner, G.; Zucchini, W.; Jaros, G.G. The electromyogram (EMG) as a control signal for functional neuromuscular stimulation. I. Autoregressive modeling as a means of EMG signature discrimination. *IEEE Trans. Biomed. Eng.* **1988**, *35*, 230–237. [CrossRef]
22. Li, X.; Zhuo, Q.; Zhang, X.; Samuel, O.W.; Xia, Z.; Zhang, X.; Fang, P.; Li, G. FMG-based body motion registration using piezoelectret sensors. In Proceedings of the 2016 38th Annual International Conference of the IEEE Engineering in Medicine and Biology Society, Orlando, FL, USA, 16–20 August 2016; pp. 4626–4629.
23. Samuel, O.W.; Asogbon, G.M.; Sangaiah, A.K.; Fang, P.; Li, G. An integrated decision support system based on ANN and Fuzzy_AHP for heart failure risk prediction. *Expert Syst. Appl.* **2017**, *68*, 163–172. [CrossRef]
24. Naderpour, H.; Mirrashid, M. Moment capacity estimation of spirally reinforced concrete columns using ANFIS. *Complex Intell. Syst.* **2020**, *6*, 97–107. [CrossRef]
25. Rainoldi, A.; Melchiorri, G.; Caruso, I. A method for positioning electrodes during surface EMG recordings in lower limb muscles. *J. Neurosci. Methods* **2004**, *134*, 37–43. [CrossRef]
26. Kim, K.S.; Choi, H.H.; Moon, C.S.; Mun, C.W. Comparison of k-nearest neighbor, quadratic discriminant and linear discriminant analysis in classification of electromyogram signals based on the wrist-motion directions. *Curr. Appl. Phys.* **2011**, *11*, 740–745. [CrossRef]
27. Oskoei, M.A.; Hu, H. Support vector machine-based classification scheme for myoelectric control applied to upper limb. *IEEE Trans. Biomed. Eng.* **2008**, *55*, 1956–1965. [CrossRef] [PubMed]
28. Hudgins, B.; Parker, P.; Scott, R.N. A new strategy for multifunction myoelectric control. *IEEE Trans. Biomed. Eng.* **2003**, *40*, 82–94. [CrossRef] [PubMed]
29. Park, S.H.; Lee, S.P. EMG pattern recognition based on artificial intelligence techniques. *IEEE Trans. Rehabil. Eng.* **1998**, *6*, 400–405. [CrossRef]
30. Du, S.; Vuskovic, M. Temporal vs. spectral approach to feature extraction from prehensile EMG signals. In Proceedings of the 2004 IEEE International Conference on Information Reuse and Integration, Las Vegas, NV, USA, 8–10 November 2004; pp. 344–350.
31. Qingju, Z.; Zhizeng, L. Wavelet de-noising of electromyography. In Proceedings of the 2006 International Conference on Mechatronics and Automation 2006, Luoyang, Henan, China, 25–28 June 2006; pp. 1553–1558.
32. Biopac Systems, Inc. Application Note 118: EMG Frequency Signal Analysis. Available online: http://www.biopac.com/Manuals/app_pdf/app118.pdf (accessed on 23 April 2020).
33. Al-Timemy, A.H.; Khushaba, R.N.; Bugmann, G.; Escudero, J. Improving the performance against force variation of EMG controlled multifunctional upper-limb prostheses for transradial amputees. *IEEE Trans. Neural Syst. Rehabil. Eng.* **2015**, *24*, 650–661. [CrossRef]
34. Khushaba, R.N.; Takruri, M.; Miro, J.V.; Kodagoda, S. Towards limb position invariant myoelectric pattern recognition using time-dependent spectral features. *Neural Netw.* **2014**, *55*, 42–58. [CrossRef] [PubMed]
35. Philipson, L. The Electromyographic Signal Used for Control of Upper Extremity Prostheses and for Quantification of Motor Blockade during Epidural Anaesthesia. Ph.D. Dissertation, Linköping University, Linköping, Sweden, 1987.

36. Samuel, O.W.; Asogbon, M.G.; Geng, Y.; Chen, S.; Feng, P.; Chuang, L.; Wang, L.; Li, G. A novel time-domain descriptor for improved prediction of upper limb movement intent in EMG-PR system. In Proceedings of the 2018 40th Annual International Conference of the IEEE Engineering in Medicine and Biology Society, Honolulu, HI, USA, 18–21 July 2018; pp. 3513–3516.
37. Samuel, O.W.; Yang, B.; Geng, Y.; Asogbon, M.G.; Pirbhulal, S.; Mzurikwao, D.; Idowu, O.P.; Ogundele, T.J.; Li, X.; Chen, S.; et al. A new technique for the prediction of heart failure risk driven by hierarchical neighborhood component-based learning and adaptive multi-layer networks. *Future Gener. Comput. Syst.* **2020**, *110*, 781–794. [CrossRef]
38. Tkach, D.; Huang, H.; Kuiken, T.A. Study of stability of time-domain features for electromyographic pattern recognition. *J. Neuroeng. Rehabil.* **2010**, *7*, 21. [CrossRef] [PubMed]
39. Geng, Y.; Samuel, O.W.; Wei, Y.; Li, G. Improving the robustness of real-time myoelectric pattern recognition against arm position changes in transradial amputees. *Biomed Res. Int.* **2017**, *2017*, 5090454. [CrossRef]
40. Zhang, X.; Li, X.; Samuel, O.W.; Huang, Z.; Fang, P.; Li, G. Improving the robustness of electromyogram-pattern recognition for prosthetic control by a postprocessing strategy. *Front. Neurorobotics* **2017**, *11*, 51. [CrossRef]
41. Samuel, O.W.; Li, X.; Fang, P.; Li, G. Examining the effect of subjects' mobility on upper-limb motion identification based on EMG-pattern recognition. In Proceedings of the 2016 Asia-Pacific Conference on Intelligent Robot Systems, Tokyo, Japan, 20–22 July 2016; pp. 137–141.
42. Zhang, J.; Williams, S.O.; Wang, H. Intelligent computing system based on pattern recognition and data mining algorithms. *Sustain. Comput. Inform. Syst.* **2018**, *20*, 192–202. [CrossRef]
43. Li, J.; Fong, S.; Wong, R.K.; Millham, R.; Wong, K.K. Elitist binary wolf search algorithm for heuristic feature selection in high-dimensional bioinformatics datasets. *Sci. Rep.* **2018**, *7*, 1–4. [CrossRef]
44. Aborokbah, M.M.; Al-Mutairi, S.; Sangaiah, A.K.; Samuel, O.W. Adaptive context aware decision computing paradigm for intensive health care delivery in smart cities—A case analysis. *Sustain. Cities Soc.* **2018**, *41*, 919–924. [CrossRef]
45. Wei, L.; Wan, S.; Guo, J.; Wong, K.K. A novel hierarchical selective ensemble classifier with bioinformatics application. *Artif. Intell. Med.* **2017**, *83*, 82–90. [CrossRef]
46. Ferreri, F.; Ponz, D.; Vollero, L.; Guerra, A.; Di, P.G.; Petrichella, S.; Benvenuto, A.; Tombini, M.; Rossini, L.; Denaro, L.; et al. Does an intraneural interface short-term implant for robotic hand control modulate sensorimotor cortical integration? An EEG-TMS co-registration study on a human amputee. *Restor. Neurol. Neurosci.* **2014**, *32*, 281–292. [CrossRef] [PubMed]
47. Asogbon, M.G.; Samuel, O.W.; Geng, Y.; Oluwagbemi, O.; Ning, J.; Chen, S.; Ganesh, N.; Feng, P.; Li, G. Towards resolving the co-existing impacts of multiple dynamic factors on the performance of EMG-pattern recognition based prostheses. *Comput. Methods Programs Biomed.* **2020**, *184*, 105278. [CrossRef] [PubMed]
48. Ma, C.; Lin, C.; Samuel, O.W.; Xu, L.; Li, G. Continuous estimation of upper limb joint angle from sEMG signals based on SCA-LSTM deep learning approach. *Biomed. Signal Process. Control* **2020**, *61*, 102024. [CrossRef]
49. Samuel, O.W.; Asogbon, M.G.; Geng, Y.; Rusydi, M.I.; Mzurikwao, Z.B.; Chen, S.; Feng, P.; Li, G. Characterizing Multiple Patterns of Motor Intent Using Spatial-Temporal Information for Intuitively Active Motor Training in Stroke Survivors. In Proceedings of the 2020 42nd Annual International Conference of the IEEE Engineering in Medicine & Biology Society (EMBC), Montreal, QC, Canada, 20–24 July 2020; pp. 3831–3834.
50. Asogbon, M.G.; Samuel, O.W.; Geng, Y.; Chen, S.; Mzurikwao, D.; Fang, P.; Li, G. Effect of window conditioning parameters on the classification performance and stability of EMG-based feature extraction methods. In Proceedings of the 2018 IEEE International Conference on Cyborg and Bionic Systems (CBS), Shenzhen, China, 25–27 October 2018; pp. 576–580.